Hindawi
International Journal of Aerospace Engineering
Volume 2020, Article ID 8894984, 12 pages
https://doi.org/10.1155/2020/8894984

Research Article

Experiences with the GPS in Unstabilized CubeSat

Pavel Kovar

Department of Radioelektronics, Faculty of Electrical Engineering, The Czech Technical University in Prague, Prague 166 27, Czech Republic

Correspondence should be addressed to Pavel Kovar; kovar@fel.cvut.cz

Received 24 May 2020; Revised 5 September 2020; Accepted 14 September 2020; Published 26 September 2020

Academic Editor: Giovanni Palmerini

The paper summarizes the experiences with the operation of the piNAV GPS receiver in a 1U unstabilized CubeSat operated on LEO orbit. piNAV L1 is a GPS receiver developed by an author for small satellite missions. The receiver is equipped with the 15 GPS L1 C/A channels and acquisition accelerator that shortens the cold start of the receiver on LEO to 65 s. The typical power consumption is 120 mW. Lucky-7 is a private 1U technological CubeSat with power budget 1 W that operates on the quasisynchronous polar orbit at altitude 520 km. One of its scientific missions is to test the operation of GPS. The space experiments proved the successful operation of the GPS receiver. The position information was available for approximately 80% of the time, where the position outage was caused by a satellite rotation and relatively long navigation signal reacquisition. The experimental data proved that the position availability can be improved by a higher-performance signal acquisition engine.

1. Introduction

This paper deals with the architecture, testing, and operation experiences of the piNAV space GPS receiver. The piNAV receiver is likely the world's first receiver that successfully operates in unstabilized CubeSat Lucky-7 of 1U size.

The project of the GPS receiver for the small satellite began in 2012 as a supporting project to a student project of a small satellite.

The application of the GPS and satellite navigation systems for position determination of the satellites exists from the beginning of the GPS operation [1, 2]. Satellite navigation is also used in other space applications, like relative positioning for satellite rendezvous and satellite swarms [3–8] and satellite attitude determination[9–11] using interferometric measurement by several antennas.

The satellite navigation with GPS system was originally designed for military navigation in the air, sea, and land. This area of application is covered as much as possible by uniform navigation signal. Nearly the same signal quality (signal level and geometry) of the GNSS systems is at the LEO (low Earth orbit). At higher orbits, there is a problem with the signal availability. As this space is not regularly covered by navigation signals, the signal is radiated by the secondary antenna beams and their levels are attenuated.

Despite this, the GPS and GNSS systems are used for navigation of the high-altitude satellites like GEO satellites [12, 13]. There are even several studies that analyse the possibility to use the GNSS for navigation of the satellites in Moon distance [14–16].

Many professional GNSS receivers for satellite navigation like ESA TOPSTAR 3000, Sentinel M-Code GPS Receiver by General Dynamics, or GPS-601 by SpaceQuest have been developed. These receivers were designed for large satellites. Lots of these receivers are multifrequency, multisystems, and multiantenna; therefore, they are very expensive, their mass is several kilograms, and power consumption is several watts or tens of watts.

Thus, navigation receivers for regular satellites are not compatible with the nano- and picosatellites because of their large size, high power consumption, and high cost. For nano- and picosatellite navigation, a specialized miniature GPS and GNSS receivers have been developed, compatible with these satellite standards. The first small satellite GPS receivers were based on Plessey chipset [17]. The other possibility is to use a commercial RF front end and to program

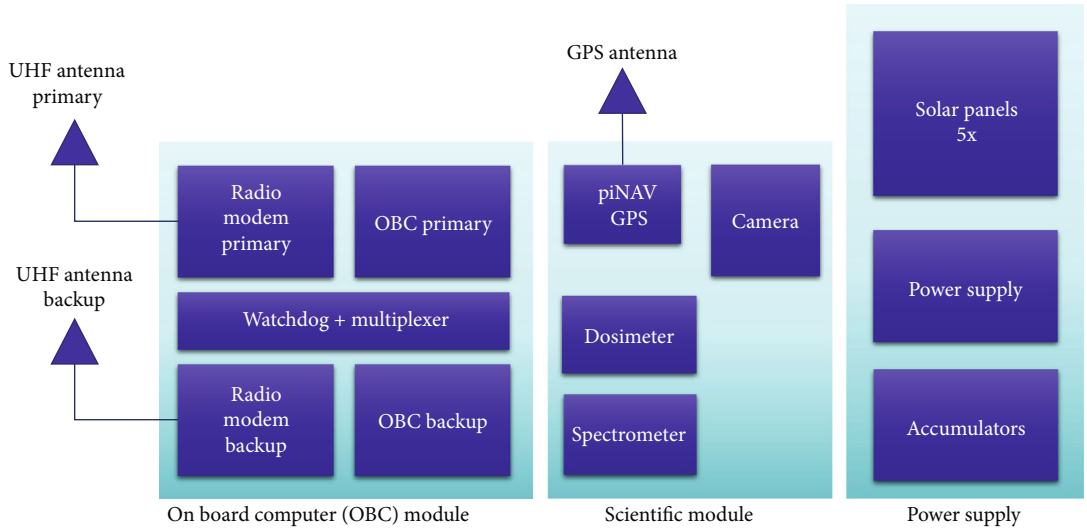

Figure 1: Simplified block diagram of Lucky-7. The satellite consists of the OBC, scientific module, power supply system, communication, and navigation antennas.

the signal processor to the FPGA. Some mass market or professional receiver manufacturers like NovaTel or uBlox [18] reprogram their receivers for small satellite navigation. The SkyTraq Technology has also adjusted its chipset for small satellite navigation.

1.1. Lucky-7 CubeSat. Lucky-7 is a 1U unstabilized satellite development by two enthusiasts Jaroslav Laifer and Pavel Kovar for the testing of electronics and GPS receiver in a real space environment. Due to the budget restriction and small development team, the satellite includes only necessary functional blocks for the fulfilment of its space mission.

The satellite (Figure 1) integrates an on-board computer (OBC) module, scientific module, power supply subsystems, two communication antennas, and one GPS antenna. The OBC module consists of two identical computers based on ARM Cortex 4 microcontroller, two UHF 2FSK radio modems of baud rate 4800 Bd, and watchdog with multiplexer circuits that serve for selection of the particular computer and monitor its operation.

The mechanical design is clear from Figure 2. The satellite frame has to protect the satellite electronics against space radiation. The radiation field in low Earth orbit (LEO) comprises a third radiation source, the Van Allen radiation belts, the product of the interaction of GCR (galactic cosmic rays), and SCR (solar cosmic rays) with the Earth magnetic field and the atmosphere. The radiation causes single event upsets of the flip flops, CMOS integrated circuits latch-ups, electronic component degradation, electrostatic charging, and human hazards.

The aluminium is a traditional material for the satellite frame design that attenuates the radiation. The attenuation of radiation in LEO by a 2 mm aluminium shield is about 100 times.

The satellite frame consists of the 1U aluminium frame covered by two-millimetre-thick aluminium panels. These panels protect the satellite electronics from the space environment, especially from the radiation. Five sides are populated by gallium arsenide solar cells, and the last panel accommodates two UHF deployable communication antennas, GPS antenna, and integrated low-resolution camera. Notice that, due to the lack of stabilization, it cannot be however given for granted that during the Lucky-7 operations, the upper hemisphere will look at the zenith, and the lower one will face the Earth.

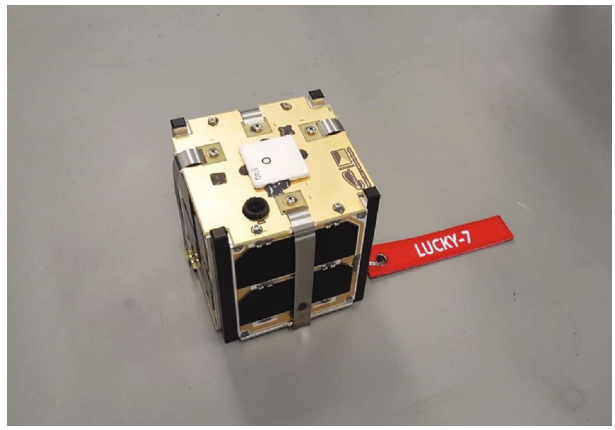

Figure 2: Photo of Lucky-7. The GPS antenna is placed at the centre of the top panel. Pair of the UHF communication antennas are wrapped. The remaining five sides are covered by solar panels.

The scientific module (Figure 3) integrates piNAV GPS receiver, radiation dosimeter and spectrometer, low-resolution camera, and other electrical and environmental sensors.

The radiation pattern of the GPS antenna is in Figure 4. It is evident that the antenna covers the upper hemisphere of the satellite while the reception from the low hemisphere is blocked by the satellite structure.

The OBC software controls the satellite, on-board scientific instruments, and communication with the ground station via UHF modem. The satellite is equipped with 2 MBs FRAM memory for the storage of the scientific data. The

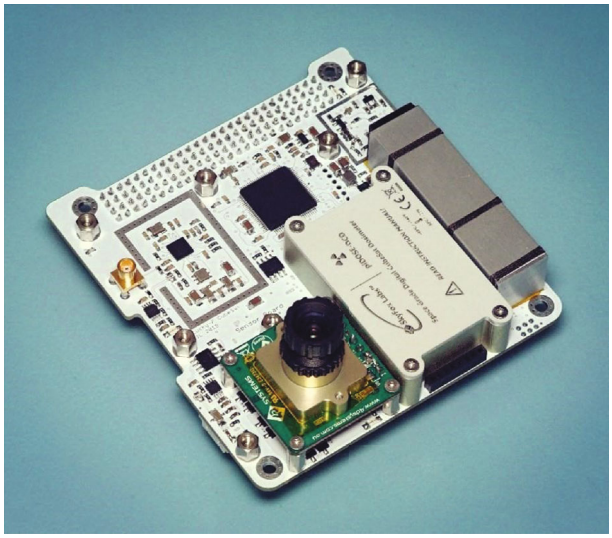

Figure 3: Scientific module. The GPS is integrated directly into the scientific board PCB. The shielding of the RF front end is removed. The module further integrates the camera, dosimeter, and spectrometer.

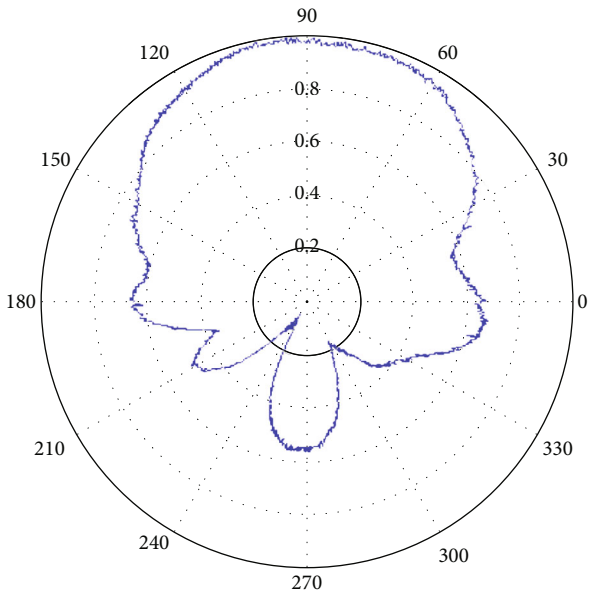

Figure 4: Measured radiation pattern of the Lucky-7 GPS antenna installed on the satellite.

memory is logically organized to blocks or cells of length 32 bytes. Each cell has a unique address. The cell's content and addresses are defined in advance. Because of the low bit rate capacity of the UHF modem, the data are stored in a highly compressed form. This fact simplifies the implementation of communication with the ground station.

The sampling rate of scientific data like dosimetry measurement or satellite status is one sample per minute. The memory length is 2048 samples which represents 34 hours of records. Data from GPS can be sampled with one second period. The length of this memory is 4096 seconds.

The communication protocol is designed for the transmission of the 32-byte cell, cell address, and CRC within a single transmission packet. The protocol implements a semi-automatic ARQ (automatic repeat request) system for communication control.

The main advantage of this communication solution is in the unequivocal interpretation of any packet; therefore, the satellite can be successfully operated even if the packet error rate is very high.

On the other hand, the satellite is very small and simple and does not integrate any Attitude Determination and Control System (ADCS) which leads to a satellite rotation effected by the Earth magnetic field and aerodynamic forces having consequently impact on the use of the satellite and UHF antennas. The satellite rotation causes the problems with the reception of the GPS satellites because the position of the GPS antenna cannot be always the optimal one. The satellite rotation also causes a problem with taking snapshots by the camera.

1.2. Satellite Orbit. Lucky-7 was launched from Vostochny Cosmodrome by Soyuz-2.1b rocket as a secondary payload on 27th June 2019. The satellite was placed to the quasi Sun-synchronous orbit of inclination 97.5° and altitude 520 km.

1.3. piNAV GPS Receiver. The design criteria of the piNAV receiver were as follows:

(i) Design of a simple GPS receiver capable of reliable operations in LEO orbit

(ii) The power consumption, size, and weight shall be compatible with the 1U CubeSat. The receiver shall consume only a fraction of the power delivered by solar cells of 1U CubeSat and occupy a fraction of the satellite volume

(iii) The receiver shall be capable of continual navigation

The development of the piNAV GPS receiver was started by a deep analysis of the receiver operation in low Earth orbit (LEO). The most critical problem that was identified is a cold start of the receiver under the Doppler shifts of the carrier frequency on LEO. The problem was analysed and simulated, and a strategy was developed for the simple GPS operation in LEO [19].

It is known that the cold start time (time to the first navigation fix after switching on the receiver without any a priori information of the time, position, and satellite constellation) of the basic receiver without the acquisition accelerator using a serial search of the acquisition space depends on the number of the receiver channels. The average cold start time of the 15 channels receiver is about 600 seconds.

The design of the receiver uses a software-defined radio (SDR) concept. The receiver is equipped with 15 early-late correlators for GPS L1 signal programmed to the low-grade FPGA, a microcontroller for correlator control and for position, velocity, and time (PVT) estimation (Figure 5). The mechanical design is clear from Figure 6. The receiver is

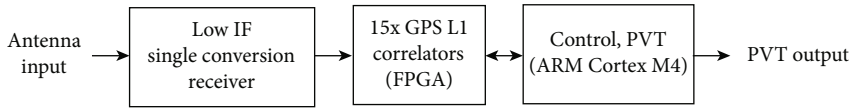

Figure 5: Block diagram of piNAV GPS receiver.

Figure 6: Photo of piNAV GPS receiver.

integrated onto a single PCB board and is equipped with RF aluminium shielding that also served for radiation protection.

2. Acquisition Unit

The signal acquisition unit calculates a coarse estimation of the Doppler frequency and code delay to be able to track the satellite signals. The acquisition of the GPS signals in LEO is complicated by a wider range of the Doppler frequency shifts.

The long cold start time appeared as the most limiting parameter of the GPS receiver; therefore, its next second and third versions (Table 1) were equipped with the signal acquisition accelerator unit [20] that shortens the acquisition time to approximately 1 minute.

The strategies of signal acquisition are shown in Figure 7. The receiver can investigate the search space serially cell by cell or use more sophisticated algorithms that calculate the cross-correlation function and replica in more points in parallel. The acquisition unit of the piNAV receiver uses a parallel search in Doppler frequency. Principle of this algorithm is in Figure 8.

Due to the small size of the FPGA of the second version, we cannot program both the GPS correlators and the acquisition unit in single device permanently. The FPGA configuration is saved in RAM and can be reprogrammed any time; therefore, these two parts are loaded consecutively. After the receiver is switched on, the receiver microcontroller programs the acquisition unit. The acquisition unit scans Doppler frequencies and code delays of all GPS satellites. After the successful acquisition of the GPS satellite signals, the FPGA is reprogrammed by GPS correlator code and the receiver starts to track the signals.

Table 1: piNAV versions.

Feature	Version I	Version II	Version III
Frequency	GPS L1 C/A		
Channel no.	15		
Acquisition	Serial	Parallel after switch on, then serial	Parallel
Cold start time	600 s	62 s	60 s
PVT	Least squares		Weighted least squares
PVT rate	1 per second, free running		1 per second, synchronized to GPS time
Real-time kernel	No		Free RTOS

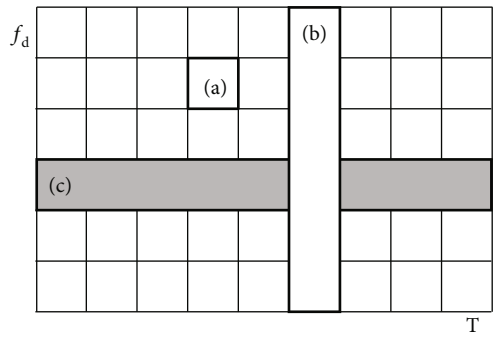

Figure 7: GPS signal acquisition methods. Single search step for (a) serial, (b) parallel in Doppler frequency, and (c) parallel in code delay approaches.

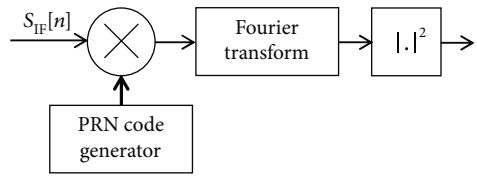

Figure 8: Simplified block diagram of the parallel acquisition method in Doppler frequency used in piNAV acquisition unit.

The advanced acquisition unit of piNAV II is available only after switching on the receiver. During following receiver operation, the serial search is implemented. The receiver uses the data from GPS almanac and precise position and time, if available, for reduction of the search space.

The piNAV III receiver is equipped with a larger FPGA that enables correlators and acquisition unit to operate at the same time. The receiver combines both acquisition methods, i.e., advanced acquisition unit and serial search with the application of the position, time, and almanac data.

Table 2: piNAV output messages.

Message	Name	Main content
$GPGGA	Global positioning system fix data	UTC, position and high in LLH, no. of tracked satellites, HDOP
$GPRMC	Recommended minimum sentence C	UTC, LLH position and high, ground speed and course
$GPVTG	Track made good and ground speed	Course and ground speed
$GPGSV	Satellites in view	Azimuth and elevation of GPS satellites and signal-to-noise ratio
$PSLSP	LEO satellite position	GPS time and week, position in ECEF, no. of sat. used for PVT, PDOP
$PSLSV	LEO satellite velocity	GPS time and week, velocity vector in ECEF, no. of sat. used for PVT, PDOP
$PSLSS	Receiver status	Power line voltage, current, antenna current, receiver temperature

When there is a successful tracking of at least six satellites, the acquisition unit is temporarily disabled for the purpose of the energy saving.

3. Output Protocol

The receiver uses a modified NMEA-0183 protocol for the provision of the position, velocity, and time information. The modification consists in stating all courses relative to the geographical North and all altitudes relative to the ellipsoid WGS84 instead of magnetic North and Geoid. In addition, three new sentences ($PSLSP, $PSLSV, and $PSLSS) have been defined (Table 2). The new messages solve the absence of the vertical velocity in standard NMEA messages and present the receiver position in a more suitable form for LEO satellite navigation that is Cartesian coordinate Earth-Centered Earth-Fixed (ECEF) instead of the standard Longitude, Latitude, and Altitude (LLA) system.

The last message carries out the receiver voltage, receiver and antenna amplifier currents, and receiver temperature for diagnostic purposes.

4. piNAV Ground Testing

The piNAV receiver was tested using a software GPS simulator ReGen [21]. GPS simulator enables to test the whole receiver by radio frequency signals that are in the LEO. The four test scenarios (static, equatorial orbit, zero meridian trajectory, and International Space Station- (ISS-) like orbit scenarios) (Figure 9) were applied [22].

The test results were analysed, and the absolute position errors were calculated from the measured position and reference position for which the test signals were generated. The example of the position errors for ISS scenario is in Figure 10. The mean values and standard deviations of the position errors for all scenarios are in Table 3.

5. Radiation Hardening Testing

The radiation hardening testing [23] was performed by a cobalt-60 source at the Institute of Nuclear Physics of the Academy of Sciences of the Czech Republic. Cobalt is a high intensive source of gamma radiation of energy 1.3 MeV that is widely used in laboratories and industry.

Let us remember that LEO radiation is considerably different from the cobalt monochromatic gamma radiation.

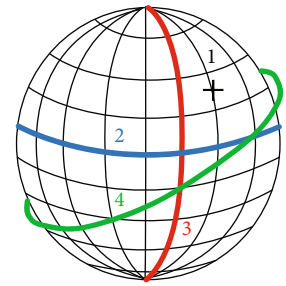

Figure 9: Test scenarios ((1) static, (2) equatorial orbit, (3) prime meridian trajectory, and (4) ISS-like orbit).

It consists not only of photons but also of protons, neutrons, and heavy particles of various energies. The sensitivity of the receiver on such radiation and radiation shield attenuation can be considerably different.

The four receivers were tested to avoid random effects and failures. Three receivers were equipped with the 2 mm aluminium case while the last receiver was uncovered. All receivers were put to the operation mode and connected to the antenna. The time for dysfunction was observed. We obtained very consistent results. Three shielded receivers persisted absorbed dose about 350 Gy and unshielded receiver 315 Gy. The differences between the shielded receivers were lower than 2 Gy.

The radiation gradually put out individual channels from operation. The receiver suddenly lost the satellite signal despite the fact that the particular satellite was visible and with the good quality of signal (signal-to-noise ratio). The channel handling routine that runs on the ARM microcontroller had detected the loss of the signal and ran the reacquisition procedure. The reacquisition procedure was firstly successful, but the signal lock was short and was gradually shortening with time of experiment. After several tens of minutes or hours, the reacquisition was not successful. The receiver finally lost all channels. The receiver failure was detected as a time in which the receiver lost the position.

The detailed analysis of the receiver data discovered the failure of the FPGA in all cases. The FPGA was found as the most sensitive part to the radiation. During the irradiation, no increasing receiver current consumption was observed.

6. Results and Discussion

This paragraph summarizes the processed data obtained from the Lucky-7 satellite. We analysed the operating

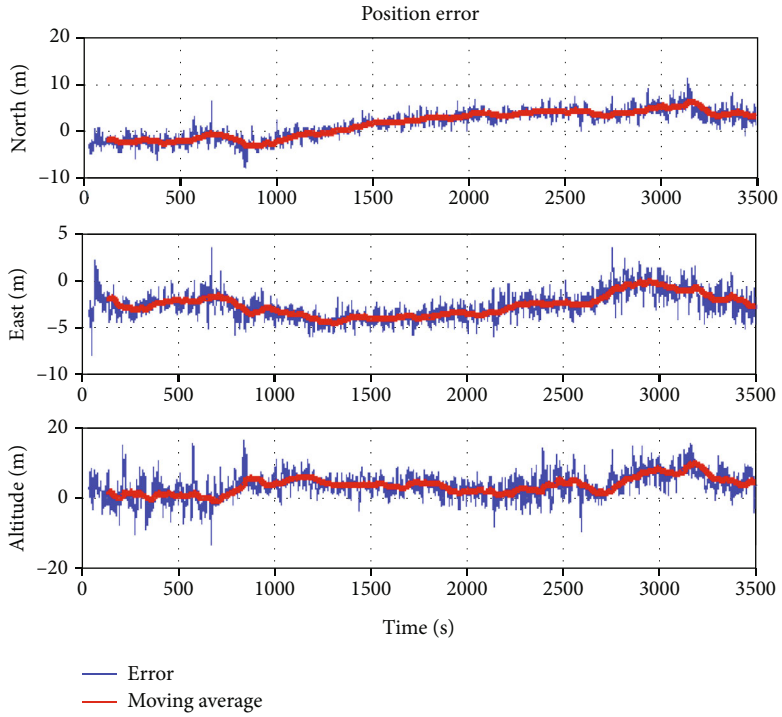

Figure 10: Position errors for ISS scenario.

Table 3: Mean values and standard deviations of piNAV position errors.

	Scenario							
	Static		Equatorial orbit		Prime meridian		ISS	
	Mean (m)	Dev. (m)	Mean (m)	Dev. (m)	Mean (m)	Dev. (m)	Mean (m)	Dev. (m)
2D	1.22	0.68	1.43	1.02	1.88	1.27	4.40	1.18
3D	1.98	1.00	4.08	2.35	4.69	2.73	6.35	2.43

conditions inside the satellite like radiation and temperature. In the next paragraph, the receiver power consumption is presented as well as the evaluation of the operation after six months in orbit. The last section presents the navigation performance like position availability, a number of the navigation satellites used for PVT, and position dilution of precision (PDOP) that measures the quality of the navigation satellite constellation used for position determination. Finally, the variation of the signal-to-noise ratio (C/N0) caused by the satellite rotation is presented.

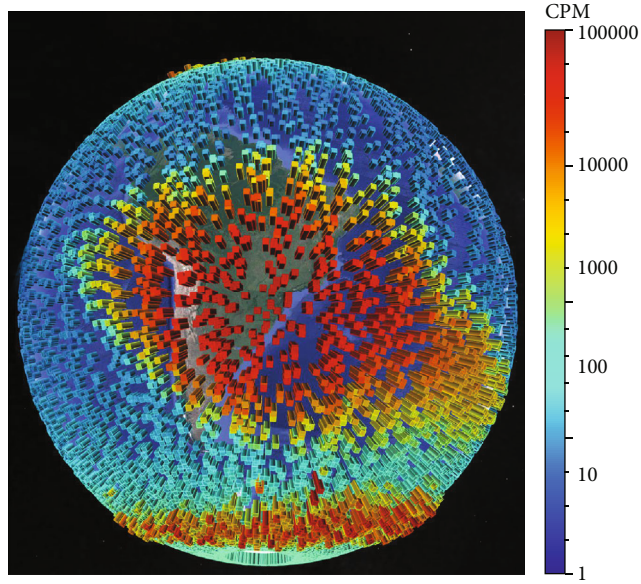

Figure 11: Radiation data measured by an onboard detector combined with the GPS position. 1 CMP~2.10^{-4} mGy/day.

7. Operation Conditions

Figure 11 shows radiation inside the satellite measured by an onboard radiation detector. The peak radiation maximum was measured in South Atlantic Anomaly where the peak absorbed dose rate reaches 24 mGy/day. The average value is 0.42 mGy/day. If we assume that radiation remains unchanged and take into account that according to the laboratory tests the unshielded receiver persists absorbed dose 315 Gy, the receiver can remain in operation 750,000 days which represents approximately 2000 years.

The receiver temperature oscillates approximately from 12 to 26°C (see Figure 12). The temperature correspondents to the solar cell's current and satellite accumulator voltage.

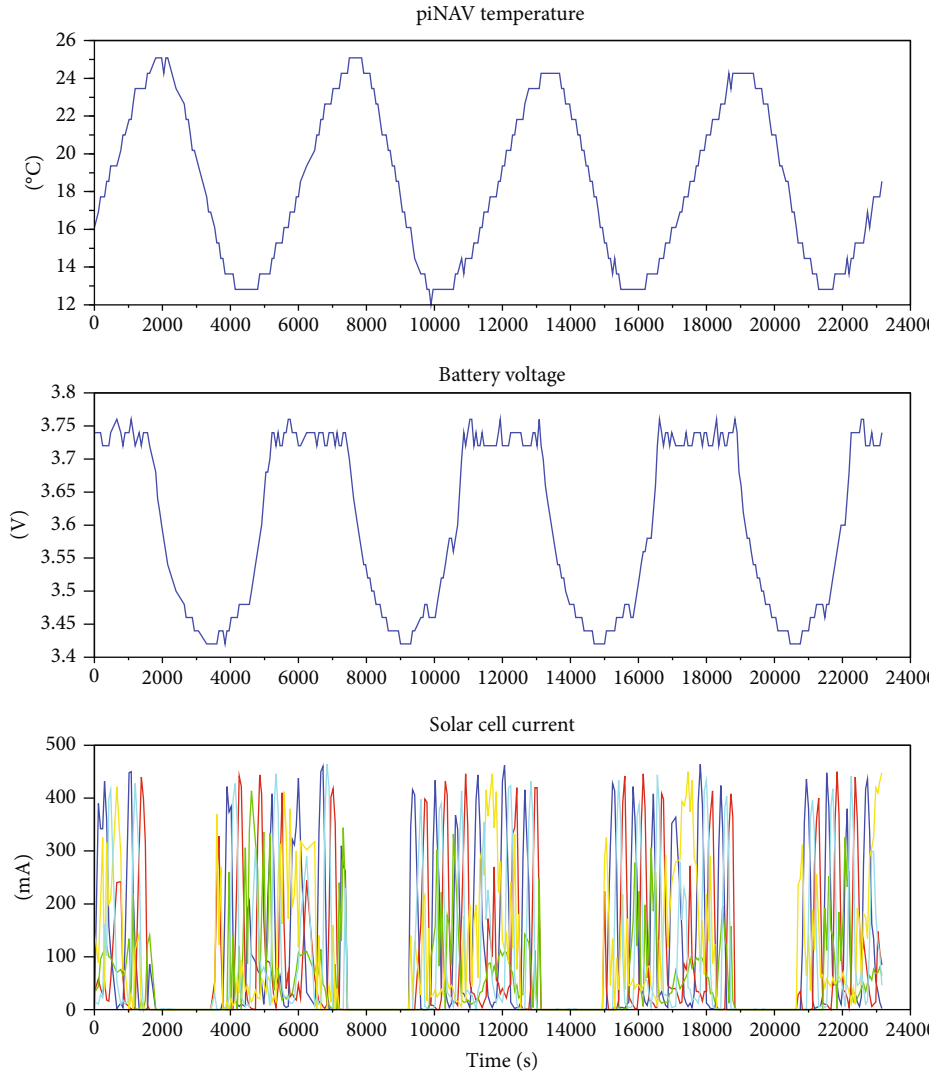

Figure 12: GPS receiver temperature and its relationship with accumulator voltage and solar cell current. Temperature is rounded to 1°C and current to 1 mA in the satellite; the current of the cells varies due to the satellite rotation.

If the satellite is illuminated by the Sun, the temperature rises, and if the satellite is in the Sun shade, the temperature drops.

8. Power Consumption

The GPS receiver and antenna power and current consumptions are the main diagnostic parameters of the piNAV receiver. As the GPS antenna with its low-noise amplifier is placed on the satellite surface, it has lower protection from the space weather than the receiver that is mounted inside; the antenna current and antenna power consumption are monitored separately.

The half-year satellite operation shows that the bus voltage and the antenna and receiver current consumption were unchanged and they stay on the initial values. The satellite bus voltage is 3.4 V, the receiver's current consumption is 42 mA, and the antenna's current consumption is 22 mA. The power consumption of the receiver is therefore 142 mW, and power consumption of the antenna is 75 mW.

9. Navigation Performance

The navigation performance was calculated from the data that was received and processed during the half-year of receiver operation. The example of one-second GPS measurement of duration 500 s is in Figure 13. The first graph displays position vector in the ECEF coordinates frame, the second one the velocity vector, and the last one development of the number of received satellites. There can be observed a problem with the satellite availability at time 440 s. The receiver tracked at first one and subsequently two satellites below 5°elevation mask. This caused alteration of the true position and default switch-on position (zero position and velocity vector). The receiver firstly detected that there were insufficient satellites above the elevation mask and blocked position and reinitiated PVT algorithms. At the next second, the reinitiated algorithm calculated a new position from all tracked satellites; because the elevation mask could not be calculated, the receiver had no position for this calculation.

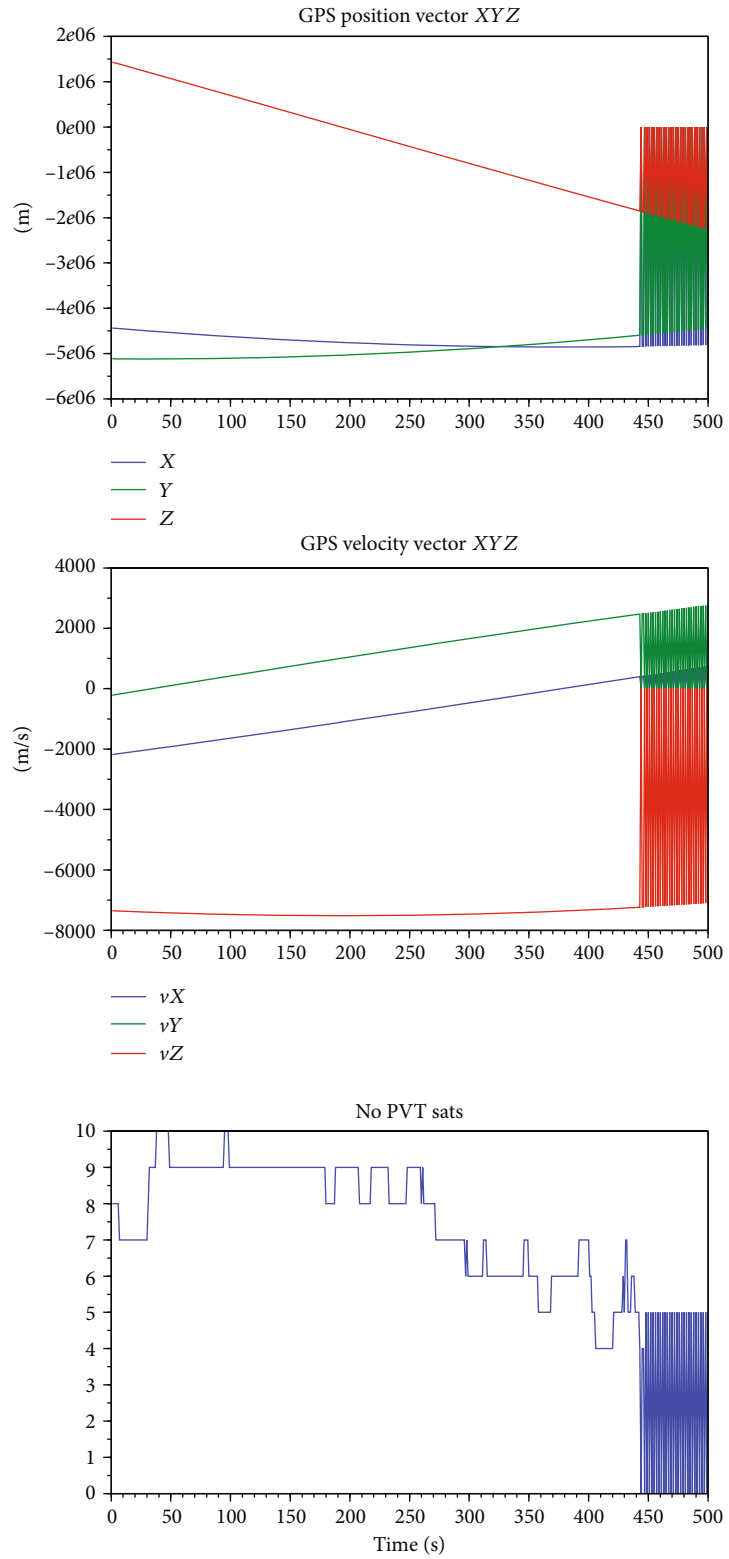

Figure 13: Example of the position and velocity 1-second measurement and development of the number of satellites.

The time development of the C/N0 of selected satellites is in Figure 14. The C/N0 is the main characteristic that measures the quality of the received signal. It is a ration of the power of the dispreaded satellite signal (carrier) and spectral power density of the noise. The level of the noise in the output of the receiver is maintained at the constant (optimal) level by an Automatic Gain Control (AGC). As the power of the satellite signal is much lower than the power of the noise, its presents in the input signal have a negligible impact on the AGC.

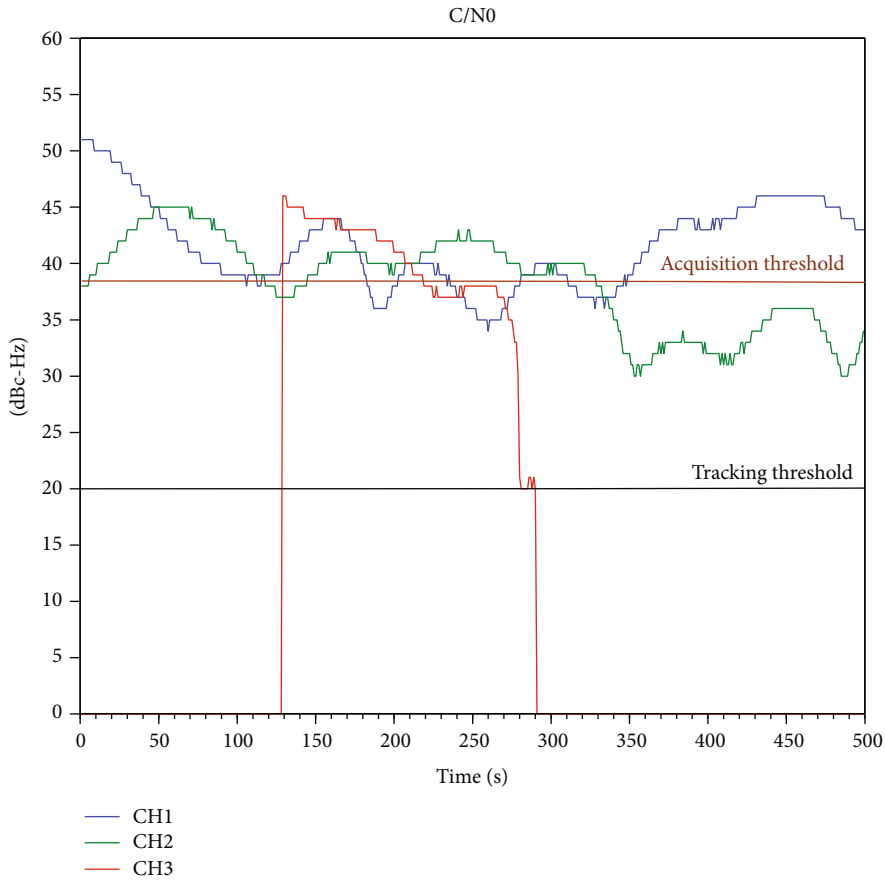

Figure 14: Development of the C/N0 of selected satellites. The oscillation is caused by a satellite rotation. The receiver uses a software tracking threshold 20 dBc-Hz. If the signal falls below this value, the reacquisition is started.

The power of the dispersed satellite signal is measured on the output of the correlator.

The C/N0 oscillation is caused by a satellite rotation. It is evident that the signal-to-noise ratio falls below the acquisition sensitivity that is 41 dBc-Hz for acquisition unit and 38 dBc-Hz for serial acquisition.

The position availability is summarized in Table 4. The position is available approximately 82% of the operation time with six satellites as an average number of satellites that were used for position, velocity, and time (PVT) calculation. Position outage is caused by the loss of signals due to the satellite rotation. The normalized histogram of the number of satellites used for position determination is in Figure 15. The normalized histogram of PDOP values that measures the quality of the navigation satellite constellation used for PVT is in Figure 16.

The performance of the acquisition unit of the piNAV version II at the satellite orbit and its comparison with the performance on the ground is in Table 5. The table summarises the relative frequency of acquisition of the given number of navigation satellites in laboratory conditions and compares them with the real measurement in the unstabilized satellite in the orbit.

The table statistics was based on 20 experiments only because of lengthy measurement related to acquisition.

Table 4: GPS receiver performance.

	Average	Min.	Max.
Position availability	82%	—	—
No. of satellites used for PVT	6	4	11
PDOP	4.4	1.1	100

It is evident that the number of successfully acquired satellites at orbit is much lower than on the ground under perfect sky visibility. The problem is mainly caused by the satellite rotation. The solution is an upgrade to the acquisition unit.

10. Conclusions

The space experiment in LEO orbit with the Lucky-7 proves that the piNAV version II can reliably operate in LEO orbit in small unstabilized 1U CubeSat. The position information and time are usable for stamping of the other physical data with precise time and position.

Due to satellite rotation, the position is not available all the time, and the navigation data availability is more than 80%. The main problem is the slow reacquisition of the signal. This problem was solved at piNAV version III that

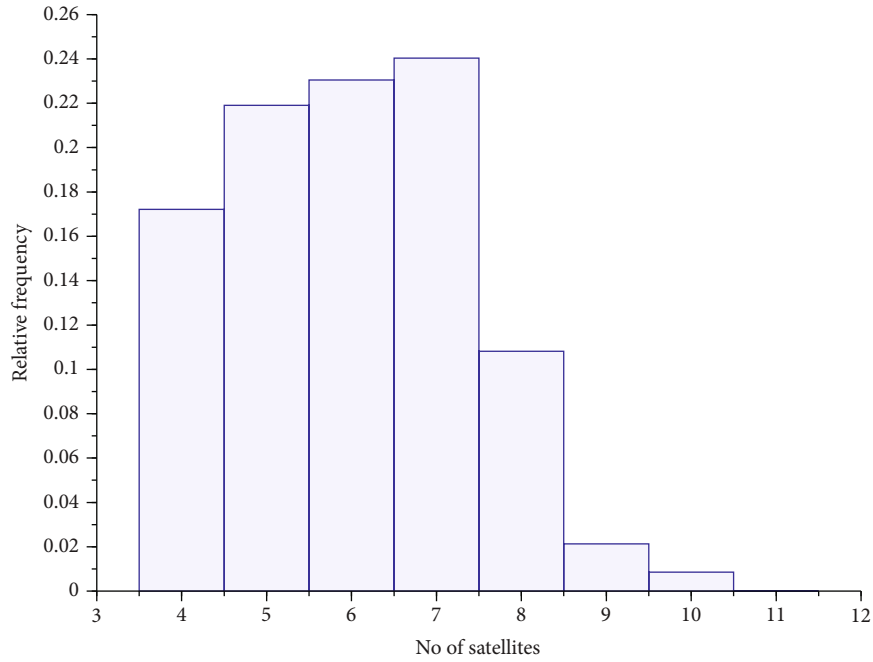

Figure 15: Normalized histogram of the number of satellites used for position, velocity, and time calculation.

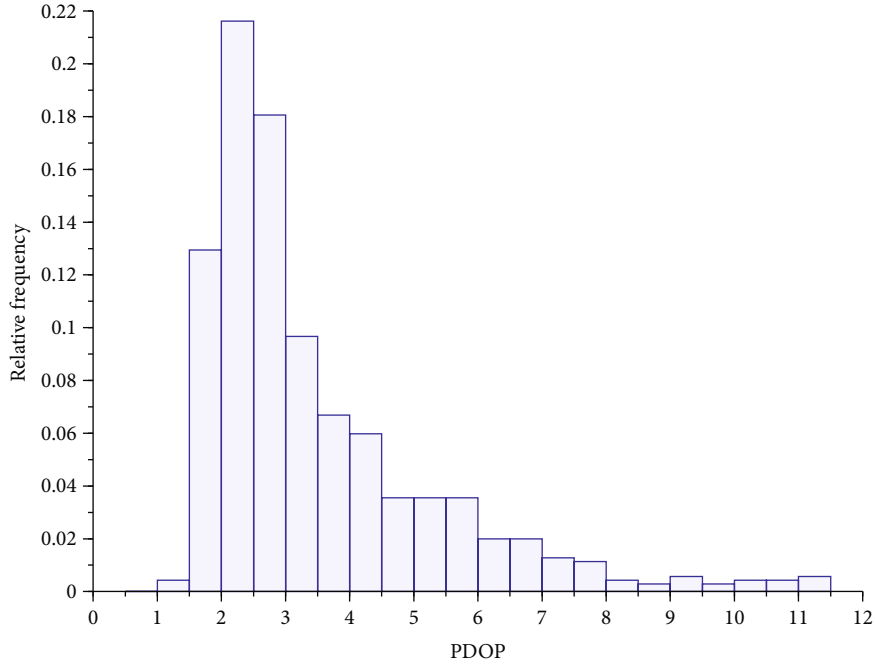

Figure 16: Normalized histogram of the PDOP. The lower the value, the better.

Table 5: Relative frequency of the acquisition of the given number of the satellites by an acquisition unit.

No. of acquired satellites	1	2	3	4	5	≥6
Ground test	—	—	5%	40%	30%	25%
CubeSat on the orbit	25%	45%	15%	5%	—	—

integrates high-performance acquisition unit based on the parallel search in Doppler frequency, which calculates data for rapid acquisition once per second.

The environment in the CubeSat in LEO orbit equipped with 2 mm thick aluminium radiation shield is suitable for long-term reliable operation of the electronics based on COTS components. The temperature of the satellite never exceeded interval 5 to 35°C. Although the average radiation dose rate is approximately 300 times higher than on the

Earth's surface, the piNAV navigation receiver has been shown to operate in this environment for many years.

The next logical step in the piNAV program is to develop a new higher-performance version. Unfortunately, the development of the space GNSS receiver for small satellites is a very complicated process that covers not only the implementation of the required signal processing algorithms but also a proper selection of the radiation tolerant components and high-reliability manufacturing process. This was successively done in piNAV II receiver thanks to a very conservative selection of the components that are more radiation tolerant than the latest high-performance ones.

The next step is the finalization of the piNAV III receiver. Unfortunately, the most problematic component that is FPGA must be upgraded. We have developed and tested a complete new acquisition unit that operates simultaneously with the correlators. The acquisition sensitivity is improved on to 36 dBc-Hz. The acquisition time of the satellite in LEO is one second. The unit can be disabled with the aim of decreasing the power consumption if it is not needed. The signal acquisition and the main reacquisition are much faster than in piNAV II.

The new version of the PVT algorithms based on the weighted least squares method was implemented. The software runs under real-time kernel and many other improvements. The receiver is in the phase of the development of the prototype and finalization of the software.

The development of the multiconstellation or multifrequency receiver for CubeSats is not currently planned because they require a higher performance but fewer radiation-tolerant FPGA.

Data Availability

Data used for the preparation of this paper is available at the author upon request.

Conflicts of Interest

The author of the manuscript has no conflict of interest to report.

Acknowledgments

The data processing and preparation of this paper was supported by the European Regional Development Fund Project CRREAT (No. CZ.02.1.01/0.0/0.0/15_003/0000481).

References

[1] W. M. Lear, "GPS navigation for low-earth orbiting vehicles," in *NASA 87-FM-2, Rev. 1, JSC-32031*, Lyndon B. Johnson Space Center, Houston, TX, USA, 1987.

[2] W. Bertiger and S. C. Wu, "Single frequency GPS orbit determination for low Earth orbiters," in *National Technical Meeting*, Institute of Navigation, Santa Monica, CA, USA, 1996.

[3] S. Cacopardi, L. Caporicci, S. Falzini, and C. Soddu, "GPS relative navigation in rendezvous operations," *Electronics Letters*, vol. 26, no. 20, pp. 1640-1641, 1990.

[4] J. Yuan, J. Luo, X. Dou, and Q. Fang, "Relative navigation for multi-spacecraft system with GPS," *IEEE Aerospace and Electronic Systems Magazine*, vol. 13, no. 12, pp. 25–28, 1998.

[5] A. Renga, M. Grassi, and U. Tancredi, "Relative navigation in LEO by carrier-phase differential GPS with intersatellite ranging augmentation," *International Journal of Aerospace Engineering*, vol. 2013, 11 pages, 2013.

[6] A. P. M. Chiaradia, H. K. Kuga, and A. F. B. de Almeida Prado, "Onboard and real-time artificial satellite orbit determination using GPS," *Mathematical Problems in Engineering*, vol. 2013, Article ID 530516, 8 pages, 2013.

[7] S. S. Hwang and J. L. Speyer, "Particle filters with adaptive resampling technique applied to relative positioning using GPS carrier-phase measurements," *IEEE Transactions on Control Systems Technology*, vol. 19, no. 6, pp. 1384–1396, 2011.

[8] Y. Yang, X. Yue, and J. Yuan, "GPS based reduced-dynamic orbit determination for low Earth orbiters with ambiguity fixing," *International Journal of Aerospace Engineering*, vol. 2015, Article ID 723414, 11 pages, 2015.

[9] X. Wang, X. Shao, D. Gong, and D. Duan, "GPS/VISNAV integrated relative navigation and attitude determination system for ultra-close spacecraft formation flying," *Journal of Systems Engineering and Electronics*, vol. 22, no. 2, pp. 283–291, 2011.

[10] L. Baroni and H. K. Kuga, "Analysis of attitude determination methods using GPS carrier phase measurements," *Mathematical Problems in Engineering*, vol. 2012, Article ID 596396, 10 pages, 2012.

[11] N. Nadarajah, P. J. G. Teunissen, and P. J. Buist, "Attitude determination of LEO satellites using an array of GNSS sensors," in *2012 15th International Conference on Information Fusion*, pp. 1066–1072, Singapore, Singapore, July 2012.

[12] L. M. B. Winternitz, W. A. Bamford, and G. W. Heckler, "A GPS receiver for high-altitude satellite navigation," *IEEE Journal of Selected Topics in Signal Processing*, vol. 3, no. 4, pp. 541–556, 2009.

[13] J. D. Kronman, "Experience using GPS for orbit determination of a geosynchronous satellite," in *Proceedings of the 13th International Technical Meeting of the Satellite Division of the Institute of Navigation (ION GPS 2000)*, pp. 1622–1626, Salt Lake City, UT, USA, 2000.

[14] H. D. Lopes, J. S. Silva, P. F. Silva et al., "GNSS-based navigation for lunar missions," in *Proceedings of the 27th International Technical Meeting of the Satellite Division of The Institute of Navigation (ION GNSS+2014)*, pp. 1536–1553, Tampa, FL, USA, 2014.

[15] M. Manzano-Jurado, J. Alegre-Rubio, A. Pellacani et al., "Use of weak GNSS signals in a mission to the moon," in *2014 7th ESA Workshop on Satellite Navigation Technologies and European Workshop on GNSS Signals and Signal Processing (NAVITEC)*, pp. 1–8, Noordwijk, Netherlands, December 2014.

[16] N. Witternigg, G. Obertaxer, M. Schoenhuber et al., "Weak GNSS signal navigation in lunar missions," in *Proceedings of the 67th International Astronautical Congress*, Jerusalem, 2015.

[17] T. Ebinuma, M. Unwin, C. Underwood, and E. Imre, "A miniaturised GPS receiver for space applications," *IFAC Proceedings*, vol. 37, no. 6, pp. 1103–1106, 2004.

[18] European Space Agency, *A Miniature CubeSat Has Become the First Satellite to Perform Galileo-Based Position Fixes in Orbit Using a Commercial Satnav Receiver*, GPS Word, 2020.

[19] P. Kovar and S. Jelen, "Cold start strategy of the CubeSat GPS receiver," *Advances in Electrical and Computer Engineering*, vol. 14, no. 2, pp. 29–34, 2014.

[20] J. Wang, X. Han, and M. Gao, "Implementation of acquisition algorithm for multi-system software-based BD/GPS receiver," in *2018 Cross Strait Quad-Regional Radio Science and Wireless Technology Conference (CSQRWC)*, pp. 1–4, Xuzhou, China, July 2018.

[21] I. Petrovski and T. Tsujii, *Digital Satellite Navigation and Geophysics; a Practical Guide with GNSS Signal Simulator and Receiver Laboratory*, Cambridge University Press, 2012.

[22] P. Kovar, "PiNAV L1—GPS receiver for small satellites," *Gyroscopy Navigation*, vol. 8, no. 2, pp. 159–164, 2017.

[23] C. Underwood, M. Unwin, R. H. Sorensen, A. Frydland, and P. Jameson, "Radiation testing campaign for a new miniaturised space GPS receiver," in *2004 IEEE Radiation Effects Data Workshop (IEEE Cat. No.04TH8774)*, pp. 120–124, Atlanta, GA, USA, July 2004.